Chemical Science

Accepted Manuscript

This is an *Accepted Manuscript*, which has been through the Royal Society of Chemistry peer review process and has been accepted for publication.

Accepted Manuscripts are published online shortly after acceptance, before technical editing, formatting and proof reading. Using this free service, authors can make their results available to the community, in citable form, before we publish the edited article. We will replace this *Accepted Manuscript* with the edited and formatted *Advance Article* as soon as it is available.

You can find more information about *Accepted Manuscripts* in the Information for Authors.

Please note that technical editing may introduce minor changes to the text and/or graphics, which may alter content. The journal's standard Terms & Conditions and the Ethical guidelines still apply. In no event shall the Royal Society of Chemistry be held responsible for any errors or omissions in this *Accepted Manuscript* or any consequences arising from the use of any information it contains.

ROYAL SOCIETY OF CHEMISTRY

www.rsc.org/chemicalscience

Chemical Science

ARTICLE

Electrochemical Buckling Microfabrication

Received 00th January 20xx,
Accepted 00th January 20xx

DOI: 10.1039/x0xx00000x

www.rsc.org/

Jie Zhang,[a] Bo-Ya Dong,[b] Jingchun Jia,[a] Lianhuan Han,[a] Fangfang Wang,[a] Chuan Liu,[a] Zhong-Qun Tian,[a] Zhao-Wu Tian,[a] Dongdong Wang*[b] and Dongping Zhan*[a]

Can isotropous wet chemical etching be controlled with a spatial resolution at nanometer scale, especially, for the repetitive microfabrication of hierarchical 3D μ-nanostructures on continuously curved surface of functional materials? We present an innovative wet chemical etching method termed as “electrochemical buckling microfabrication”: First, a constant contact force is applied to generate hierarchical 3D μ-nanostructure on mold electrode surface through buckling effect; then, the etchant is on-site electrogenerated and confined close to the mold electrode surface; finally, the bulcking hierarchical 3D μ-nanostructures are transferred onto the surface of $Ga_xIn_{1-x}P$ coated GaAs wafer through WCE. The concave microlens with Fresnell structure has an enhanced photoluminescence at 630 nm. Comparing with energy beam direct writing techniques and nanoimprint lithography, it provides an electrochemical microfabrication way for semiconductor industry with low cost and high throughput.

Introduction

Microfabrication is the up-to-date theme and plays a crucial role in industrial revolution, such as ultra large scale integrated circuits[1], precision optics[2], microelectromechanical systems[3], and miniaturized total analytical systems[4, 5]. Nevertheless, great challenge is remained to fabricate hierarchical three-dimension micro- and nano-structures (3D μ-nanostructures) directly on functional materials with continuously curved surface, e.g., the artificial compound eye in optics. Photolithography is difficult to do so due to the rectilinear propagation of light.[6] Direct writing techniques based on electron beam[7], ionic beam[8] or laser beam[9, 10] are capable of fabricating 3D μ-nanostructures. However, the huge workload, high cost and serious surface damage hinder their applications in repetitive manufacturing.[11] Besides the difficulty of mold preparation, nanoimprint works only with thermoplastic or photocurable materials, which are usually not the aimed functional materials.[12, 13] Thus, it is essential to develop new principles and methods to meet the increasing demands of hierarchical 3D μ-nanostructures in industrial microfabrication.

Wet chemical etching (WCE) is one of the first techniques introduced in microfabrications.[14, 15] Proceeding along the special crystal plane, nanostructures made by anisotropic WCE on the surface of single crystalline materials are facet-dependent.[16, 17] The spatial resolution of isotropous WCE is ruined by the same etching rate in all directions.[18, 19] The common disadvantage of them is the uncontrollable process. Either over-etching or less-etching would harm the product consistency. That’s why, in semiconductor industry, WCE is now underused as a wafer cleaning process.

How to control WCE process? For years we have developed confined etchant layer technique (CELT) to solve the problem:[20-24] Firstly, the etchant is generated on the surface of mold electrode by electrochemical reaction. Secondly, the diffusion distance of the etchant is confined to micron or nanometer scale by a subsequent homogeneous reaction. Consequently, a confined etchant layer (CEL) is formed on mold electrode surface (Fig. S1 in ESI). When the CEL contacts with the workpiece by a nanomanipulation system, WCE begins. Most importantly, the WCE process will stop automatically if the workpiece material is removed and, therefore, separated from the CEL. In the case of $Ga_xIn_{1-x}P$ substrate (for GaAs it has been well discussed elsewhere[14]), the CELT strategies are formulated as followed:

The generation reaction of etchant:

$$18\,Br^- \rightarrow 9\,Br_2 + 18\,e^- \quad (1)$$

The confining reaction of etchant:

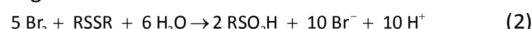

$$5\,Br_2 + RSSR + 6\,H_2O \rightarrow 2\,RSO_3H + 10\,Br^- + 10\,H^+ \quad (2)$$

The WCE reaction:

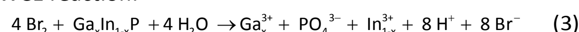

$$4\,Br_2 + Ga_xIn_{1-x}P + 4\,H_2O \rightarrow Ga_x^{3+} + PO_4^{3-} + In_{1-x}^{3+} + 8\,H^+ + 8\,Br^- \quad (3)$$

where, RSSR is L-cystine. If the concentration of L-cystine is much higher than etchant precursor, the thickness of CEL can be estimated simply by the following equation[25]:

$$\mu = \left(D/K_s\right)^{1/2} \quad (4)$$

a. State Key Laboratory of Physical Chemistry of Solid Surfaces, and Department of Chemistry, College of Chemistry and Chemical Engineering, Xiamen University, Xiamen, 361005, China. E-mail: dpzhan@xmu.edu.cn
b. College of Architecture and Civil Engineering, Xiamen University, Xiamen, 361005, China. E-mail: ddwang@xmu.edu.cn

† Electronic Supplementary Information (ESI) available: Detailed fundamentals of CELT, ECBM experiments, FEM simulation and PL image. See DOI: 10.1039/x0xx00000x

Chemical Science Accepted Manuscript

Please do not adjust margins

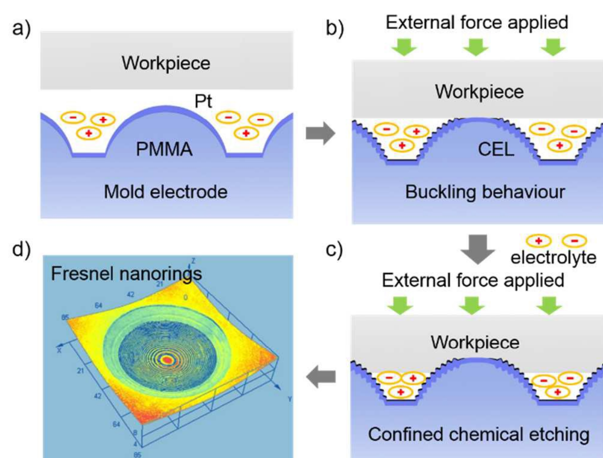

Fig. 1 Schematic illustration of the ECBM process. (a) The workpiece is approaching to the PMMA/Pt working electrode with convex microlens array. (b) When the workpiece contacts with the PMMA/Pt working electrode, a constant contact force is applied to produce hierarchical Fresnel nanostructure on the surface of microlens through buckling. Then the PMMA/Pt working electrode is biased at 1.0 V (vs. SCE) to generate the confined etchant layer. (c) With the confined wet chemical etching going on, the concave microlens with hierarchical Fresnel nanostructures are transferred on the workpiece. (d) The obtained hierarchical 3D μ-nanostructures through ECBM.

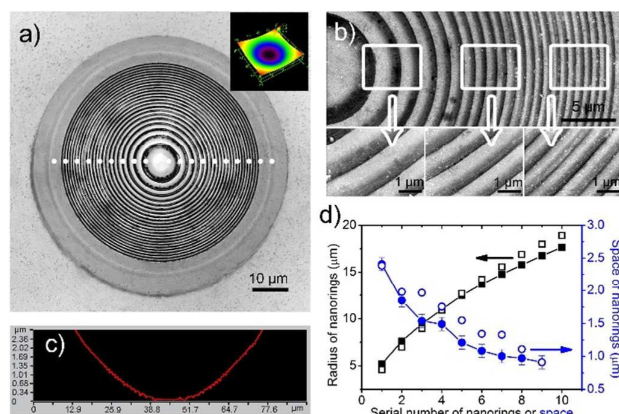

Fig. 2 Hierarchical Fresnel nanostructures fabricated through ECBM on $Ga_xIn_{1-x}P$ workpiece with 20 mN contact force. (a) Confocal laser microscope image showing 23 concentric nanorings. Inset is its 3D image. (b) High-resolution SEM images of the nanorings. (c) Topography profile of (a). (d) The change of radius and space as a function of the first ten nanorings from centre to outside. Solid symbol with eyeliner is the experimentally determined radius and space. Open symbol represents the FEM simulated results.

where μ is the thickness of CEL, D is the diffusion coefficient of etchant, K_s is the quasi-first-order rate constant of the confining reaction. If D and K_s were 10^{-5} cm^2 s^{-1} and 10^9 s^{-1}, the thickness of CEL would be ~1 nm. That means, theoretically, CELT is a very precise microfabrication method. In this way, the WCE process is well controlled at micron or nanometer scale.

How to generate hierarchical 3D μ-nanostructures and transfer them onto functional materials? Buckling is a natural phenomenon that denotes a geometric instability for a given structure under compression or shear stresses.[26] Recently, buckling effect arouses extensive interests in fabricating 3D μ-nanostructures[27-35]. By introducing elastic buckling into CELT, as depicted in Fig. 1, we develop a method termed as electrochemical buckling microfabrication (ECBM). When a constant contact force is applied between the workpiece and mold electrode, orderly hierarchical 3D μ-nanostructures are formed on the surface of convex microlens through buckling effect due to the difference of elastic modulus between the rigid platinum (Pt) film and the plastic polymethylmethacrylate (PMMA) substrate (Fig. S2). Then, the buckling 3D μ-nanostructures are transferred onto the surface of $Ga_xIn_{1-x}P$ thin film coated GaAs wafer by CELT.

Results and discussion

Fabrication of microlens with hierarchical Fresnel nanorings

In ECBM, the working electrolyte is an aqueous solution containing 0.1 M KBr, 0.1 M L-cystine and 0.5 M H_2SO_4. With a Pt counter electrode, a saturated calomel reference electrode (SCE) and an applied potential of 1.0 V at mold electrode (working electrode), bromine (Br_2) is generated to start the WCE process. Fig. 2a and 2b show the confocal laser microscopic images of the hierarchical Fresnel structure (i.e., concentric nanorings) on the concave microlens obtained with a constant contact force of 20 mN. The center nanoring has a height of 50 nm and decays also from center to outside (Fig. 2c and Fig. S3). From Fig. 2d, it is observed that, from center to outside, the radius of the first ten nanorings increases gradually from 5.2 μm to 17.7 μm while the gap between neighbor nanorings decreases from 2.4 μm to 900 nm. In the control experiment which workpiece do not contact with mold electrode, concave microlens without nanorings are fabricated (Fig. S4). The buckling nanorings on mold electrode disappears when the contact force is released. This elastic buckling behavior can avoid tool wear and make ECBM work repetitively, noting that tool wear is a serious probem for nanoimprint lithograhy for mass production.

The hierarchical Fresnel structure on concave microlens are tunable by the applied contact force. Fig. 3 shows the Fresnel structures fabricated with different contact force of 60 mN, 40 mN, 20 mN, 10 mN. The radius of the first nanoring increases from 4.9 μm to 16.7 μm with the increasing contact force (Fig. 3e). Because the mold electrode is compressed tightly on the workpiece, buckling doesn't occur in the central contact area. The larger the applied force is, the larger central area will be obtained. Moreover, the Fresnel structure become denser when the applied force increases. Gap between the first two nanorings decreases from 2.5 μm to 900 nm when the contact force changes from 10 mN to 60 mN. Although the gap between neighbor nanorings decreases from center to outside, they tends to be more uniform with increasing contact force (Fig. 3f and Fig S5).

Simulation of the buckling behaviour on mold electrode

Experimentally, we obtain buckling 3D μ-nanostructures on continueously curved surface and transfer them onto functional materials. Now we discuss the buckling effect with finite element method (FEM) by high-fidelity ANSYS finite element package.[36] Since the mold electrode is composed of a PMMA convex microlens array coated with a thin Pt film, the geometry and mechanical properties used in simulation are shown in Fig. 4a. The Young's modulus of Pt film and PMMA

Chemical Science Accepted Manuscript

This journal is © The Royal Society of Chemistry 20xx
Please do not adjust margins

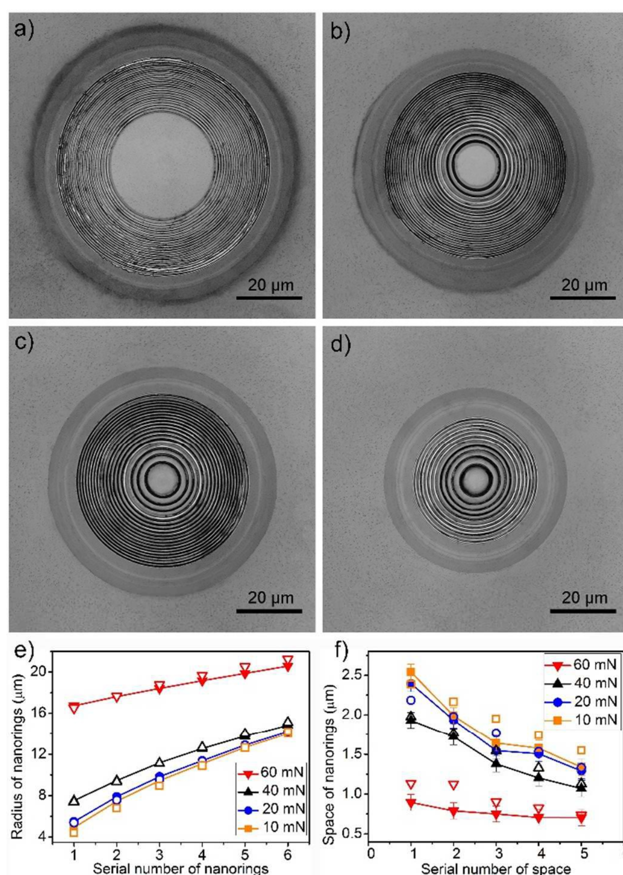

Fig. 3 Confocal laser microscope images of the hierarchical Fresnel nanostructures fabricated by ECBM with different contact force. a) 60 mN. b) 40 mN. c) 20mN. d) 10 mN. The change of radius e) and space f) as a function of the first six nanorings from centre to outside at different contact force. Solid symbol with eyeliner is experimentally determined radius and space. Open symbol is the FEM simulated results.

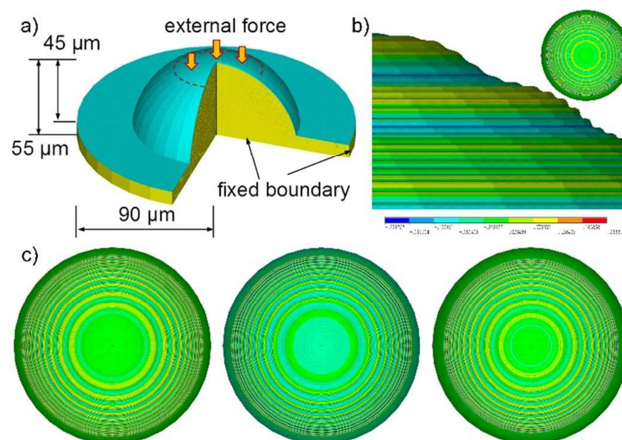

Fig. 4 Finite element simulation results of the buckling behavior at convex microlens. a) The geometric properties and boundary conditions of the model established. b) The side view of buckling patterns at 20 mN contact force. Hierarchical nanorings are formed on the surface of microlens. The inset shows the top view of buckling microlens. c) Top view of the nanorings buckled at different contact force: 60 mN, 40 mN and 10 mN from left to right.

substrate are 168 GPa and 20 Gpa (See S9) while the Poisson's ratios are 0.38 and 0.4, respectively. Both Pt film and PMMA microlens are modeled as elastic materials. The Saint-Venant type of constitutive equation is employed to relate the stress and strain tensors as follows:

$$S_{ij} = C_{ijkl}E_{kl},\ C_{ijkl} = \frac{Ev}{(1+v)(1-2v)}\delta_{ij}\delta_{kl} + \frac{E}{2(1+v)}(\delta_{ik}\delta_{jl} + \delta_{il}\delta_{jk}) \quad (5)$$

where C_{ijkl} is the elastic tensor, δ_{ij} is the Kronecker delta tensor, E and v represent the Young's modulus and Poisson's ratio. In simulations, the thickness of Pt film on PMMA convex micro-lens is non-uniform (changing gradually from 248 nm at the top to 30 nm at the bottom, See S10), which often happens in sputter coating on 3D structures. More details of FEM simulations plaese check section 6.2 in ESI..

When a contact force is applied on the mode electrode, the Pt film suffers compressive stress and passes it to the PMMA substrate. If the compressive stress exceeds the critical buckling stress, the equilibrium of the system is interrupted and buckling 3D μ-nanostructures appears due to initial imperfection or small perturbation. The buckling instability leads to the generation of hierarchical Fresnel structure on the continuously curved convex microlens. Fig. 4b shows the buckling behaviour of the mold electrode with a constant contact force of 20 mN. The gap between nanorings decreases from center to outside, which is mostly attributed to the non-uniform thickness of Pt film and the distribution of stress states on the convex microlens. The thicker film on the top of convex microlens has larger bending rigidity and yields sparser nanorings[26, 37]. On the contrary, the thinner film at the bottom results in denser nanorings. Thus, the gap between nanorings is related to the thickness distribution of Pt film on the PMMA microlens, which also provide a way for tuning the bulcking 3D μ-nanostructures.

Simulations demonstrate the buckling 3D μ-nanostructures are influenced also by the applied contact force. As shown in Fig. 4c, the gap between neighbour nanorings decreases with the increased compression. In the conventional case of planar film, larger compressive stress leads to produce smaller wavelength of buckling.[38] However, for the Pt film coated on the PMMA convex microlens discussed herein, the compressive stress in Pt film reduces gradually from top to bottom (Fig. S6). The increasing contact force leads to larger compressive stress, which results in denser buckling nanorings (Section 6.3 in ESI). FEM simulations show that the distribution of bending rigidity and compressive stress of the Pt film coated on the convex micolens plays an opposite effect on the density of nanorings, i.e., the nanorings tend to become more uniform with the increasing contact force (Fig. 4c). More discussion please check section 6.3 in ESI.

Photoluminescence of the microlens

Since the workpiece is a GaAs wafer coated with a thin $Ga_xIn_{1-x}P$ layer with a thickness of 5 μm, the outside area of the obtained concave microlens is $Ga_xIn_{1-x}P$, the central area is GaAs, and a transition region between them. In fact, each concave microlens with hierarchical Fresnel nanostructures is a semiconductor light-emitting diode (LED) with a quantum-well structure. Besides the photoelectric properties, the microlens has a structure-dependent, enhanced photoluminescence (PL) property. When the microlens shown in Fig. 5a is illuminated by a 532-nm-wavelength laser, a gradient and circular PL belt

Chemical Science Accepted Manuscript

Please do not adjust margins

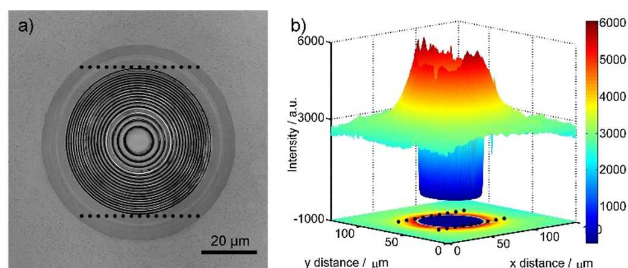

Fig. 5 The photoluminescence of the concave microlens with hierarchically concentric nanorings: a) The confocal laser image of single microlens. b) The corresponding photoluminescence image at 630-nm wavelength.

can be detected with a single-wavelength at 630 nm. The PL intensity is enhanced in the narrow outside area and quenched in the central area, i.e., the incident light is sufficiently trapped by the hierarchical Fresnel nanostructures on the concave microlens. The results illustrate that ECBM has prospective applications in semiconductor LEDs and optical microdevices. The PL images of single concave microlenses with hierarchical Fresnel nanostructures obtained at different contact force are shown in Fig. S9.

Conclusions

In conclusion, an electrochemical buckling microfabrication method is developed by introducing physical modulations into confined wet chemical etching: elastic buckling, a physical self-assembly behavior, is adopted to generate the hierarchical 3D μ-nanostructures on continuously curved surface, which are then transferred onto functional materials by confined etchant layer technique. The fabricated concave microlens with hierarchical Fresnel nanostructures has an excellent structure-dependent photoluminescences. Besides the hierarchical nanorings, parallel nano-grooves are also fabricated on the surface of concave hemicylinder (Fig. S10). Comparing with nanoimprint and energy beam direct-writing techniques, ECBM provides a controllable, high-efficient and low-cost electrochemical approach to the fabrication of semiconductor devices with hierarchical 3D μ-nanostructures.

Experimental Section

Sample preparation

All the used chemicals (KBr, H_2SO_4, L-cystine) are analytical grade or better and provided by Sinopharm Co., China. PMMA is purchased from Mitsubishi Rayon Co., Japan. The $Ga_xIn_{1-x}P$ wafers are gift from Prof. Jingqiu Liang at Changchun Institute of Optics, Fine Mechanics and Physics, Chinese Academy of Science. All solutions are prepared with deionized water (18.2 MΩ, Milli-Q, Millipore Corp.).

Fabrication of mold electrode

The concave microlens array on titanium plate (diameter: 110 μm, height: 45 μm) are imprinted onto PMMA substrate by a hot embossing technique. After cooling, the PMMA substrate is immersed in a solution of 50 g/L Na_3PO_4, 25 g/L Na_2CO_3 and 20 g/L NaOH at 85 °C for 2.5 h to remove the oil. Thin films of titanium (thickness: 5 nm) and platinum are sputtered onto the PMMA mode successively to produce the conductive mold electrode.

Electrochemical buckling microfabrication

A home-made instrument (Fig. S1d) is used to perform the ECBM. The mold electrode is fixed and approached to the workpiece by a nano-manipulator. A force sensor is used to monitor the contact force between the mold electrode and the workpiece. After the buckling 3D μ-nanostructures is generated on mold electrode, an electrochemical workstation (CHI 660D, CHI Instrument Co., USA) is used to perform CELT process. A Pt wire and a SCE is used as the counter electrode and reference electrode. The mold electrode is biased to 1.0 V to generate the etchant bromine. L-cystine is added to form CEL. During the etching process, the contact force keeps constant.

Characterizations and measurements

Confocal laser microscope (Olympus 4000, Olympus Co., Japan), scanning electron microscope (Hitachi S-4800, Hitachi High-Technologies Co., Japan), atomic force microscopy (Nanoscope III scanning probe microscope, Digital Instrument Co., USA) are employed to characterize the hierarchical 3D μ-nanostructures. Nanophoto (laser Raman microscope RAMAN-11) in a fast line scanning mode with a 50× objective (NA = 0.45), 300 lines/mm grating and 532-nm-wavelength laser (power: 0.029 mW) is employed to characterize the Photoluminescence of nanorings.

Acknowledgements

Jie Zhang and Bo-Ya Dong contributed equally. The financial support of the National Natural Science Foundation of China (91323303, 21327002, 51205333, 11222221, 21321062 and 11472233), the Natural Science Foundation of Fujian Province of China (2012J06004, 2014J06001), the Fundamental Research Funds for the Central Universities (2010121022, 2010121073, 20720150163), and the Program for New Century Excellent Talents in University (NCET-12-0318) are appreciated.

References

1 Y. Shacham-Diamand, T. Osaka, M. Datta and T. Ohba, *Advanced nanoscale ULSI interconnects: fundamentals and applications*, Springer, New York, 2009.
2 H. P. Herzig, *Micro-optics: Elements, systems and applications*, Taylor & Francis Ltd., London, 1997.
3 S. E. Lyshevski, *MEMS and NEMS: systems, devices, and structures*, Taylor & Francis Ltd., London, 2002.
4 A. Manz, N. Graber and H. M. Widmer, *Sens. Actuators, B*, 1990, **1**, 244-248.
5 T. Vilkner, D. Janasek and A. Manz, *Anal. Chem.*, 2004, **76**, 3373-3386.
6 B. D. Gates, Q. Xu, M. Stewart, D. Ryan, C. G. Willson and G. M. Whitesides, *Chem. Rev.*, 2005, **105**, 1171-1196.
7 S. J. Randolph, J. D. Fowlkes and P. D. Rack, *Crit. Rev. Solid. State.*, 2006, **31**, 55-89.

This journal is © The Royal Society of Chemistry 20xx

Chemical Science Accepted Manuscript

8 I. Utke, P. Hoffmann and J. Melngailis, *J. Vac. Sci. Technol. B*, 2008, **26**, 1197-1276.
9 B. H. Cumpston, S. P. Ananthavel, S. Barlow, D. L. Dyer, J. E. Ehrlich, L. L. Erskine, A. A. Heikal, S. M. Kuebler, I. Y. S. Lee, D. McCord-Maughon, J. Qin, H. Rockel, M. Rumi, X.-L. Wu, S. R. Marder and J. W. Perry, *Nature*, 1999, **398**, 51-54.
10 Y. L. Zhang, Q. D. Chen, H. Xia and H. B. Sun, *Nano Today*, 2010, **5**, 435-448.
11 P. T. Mannion, J. Magee, E. Coyne, G. M. O'Connor and T. J. Glynn, *Appl. Surf. Sci.*, 2004, **233**, 275-287.
12 L. J. Guo, *Adv. Mater.*, 2007, **19**, 495-513.
13 E. A. Costner, M. W. Lin, W. L. Jen and C. G. Willson, *Annu. Rev. Mater. Res.*, 2009, **39**, 155-180.
14 J. M. Bustillo, R. T. Howe and R. S. Muller, *Proc. IEEE*, 1998, **86**, 1552-1574.
15 G. T. Kovacs, N. I. Maluf and K. E. Petersen, *Proc. IEEE*, 1998, **86**, 1536-1551.
16 B. Li, M. K. Kang, K. Lu, R. Huang, P. S. Ho, R. A. Allen and M. W. Cresswell, *Nano Lett.*, 2007, **8**, 92-98.
17 Y. Y. Zhang, J. Zhang, G. Luo, X. Zhou, G. Y. Xie, T. Zhu and Z. F. Liu, *Nanotechnology*, 2005, **16**, 422.
18 D. R. Turner, *J Eelctrochem. Soc.*, 1958, **105**, 402-408.
19 H. Robbins and B. Schwartz, *J Eelctrochem. Soc.*, 1959, **106**, 505-508.
20 Z. W. Tian, Z. D. Fen, Z. Q. Tian, X. D. Zhuo, J. Q. Mu, C. Z. Li, H. S. Lin, B. Ren, Z. X. Xie and W. L. Hu, *Faraday Discuss.*, 1992, **94**, 37-44.
21 L. Zhang, X. Z. Ma, J. Tang, D. S. Qu, Q. Y. Ding and L. N. Sun, *Electrochim. Acta*, 2006, **52**, 630-635.
22 X. Z. Ma, L. Zhang, G. H. Cao, Y. Lin and J. Tang, *Electrochim. Acta*, 2007, **52**, 4191-4196.
23 L. Zhang, X. Z. Ma, J. L. Zhuang, C. K. Qiu, C. L. Du, J. Tang and Z. W. Tian, *Adv. Mater.*, 2007, **19**, 3912-3918.
24 Y. Yuan, L. H. Han, J. Zhang, J. C. Jia, X. S. Zhao, Y. Z. Cao, Z. J. Hu, Y. D. Yan, S. Dong, Z. Q. Tian, Z. W. Tian and D. P. Zhan, *Faraday Discuss.*, 2013, **164**, 189-197.
25 A. J. Bard and L. R. Faulkner, *Electrochemical Methods: Fundamentals and Applications*, Wiley, New York, 2 edn., 2001.
26 L. D. Landau, E. M. Lifshitz, A. M. Kosevich and L. P. Pitaevskiĭ, *Theory of Elasticity*, Butterworth-Heinemann, Oxford, 3 edn., 1986.
27 N. Bowden, S. Brittain, A. G. Evans, J. W. Hutchinson and G. M. Whitesides, *Nature*, 1998, **393**, 146-149.
28 A. L. Volynskii, S. Bazhenov, O. V. Lebedeva and N. F. Bakeev, *J. Mater. Sci.*, 2000, **35**, 547-554.
29 J. S. Sharp and R. A. L. Jones, *Adv. Mater.*, 2002, **14**, 799-802.
30 P. J. Yoo, K. Y. Suh, S. Y. Park and H. H. Lee, *Adv. Mater.*, 2002, **14**, 1383-1387.
31 K. Efimenko, M. Rackaitis, E. Manias, A. Vaziri, L. Mahadevan and J. Genzer, *Nature Mater.*, 2005, **4**, 293-297.
32 E. P. Chan and A. J. Crosby, *Adv. Mater.*, 2006, **18**, 3238-3242.
33 C. Lu, H. Möhwald and A. Fery, *Chem. Mater.*, 2008, **20**, 7052-7059.
34 N. Pazos-Pérez, W. Ni, A. Schweikart, R. A. Alvarez-Puebla, A. Fery and L. M. Liz-Marzán, *Chem. Sci.*, 2010, **1**, 174-178.
35 S. Yang, K. Khare and P. C. Lin, *Adv. Funct. Mater.*, 2010, **20**, 2550-2564.
36 O. C. Zienkiewicz and R. L. Taylor, *The Finite Element Method For Solid And Structural Mechanics*, Butterworth-Heinemann, Oxford, 6 edn., 2005.
37 E. Cerda and L. Mahadevan, *Phys. Rev. Lett.*, 2003, **90**, 074302.
38 H. Jiang, D. Y. Khang, J. Song, Y. Sun, Y. Huang and J. A. Rogers, *Proc. Natl. Acad. Sci. U.S.A.*, 2007, **104**, 15607-15612.

Chemical Science Accepted Manuscript